Diffusion in liquid alkali metals



1994 J. Phys.: Condens. Matter 6 1309

(http://iopscience.iop.org/0953-8984/6/7/004)

J. Phys.: Condens. Matter 6 (1994) 1309–1318. Printed in the UK

# Diffusion in liquid alkali metals

S Ranganàthan and K N Pathak†

Department of Mathematics and Computer Science, Royal Military College, Kingston, Ontario, Canada K7K 5LO

Received 8 September 1993, in final form 15 November 1993

**Abstract.** A simple model of atomic motion has been used to calculate the velocity auto-correlation function, its frequency spectrum, the associated memory function, and the self-diffusion coefficients for liquid alkali metals. There are no adjustable parameters in the model and the only inputs required are the interatomic potential and the pair correlation function. The predicted results are in good agreement with recent computer simulation data. The self-diffusion coefficients are found to be very close to actual experimental values for all liquid alkaline metals, including lithium, and they seem to scale, the scaling being determined by energy and length parameters for the interatomic potential and the mass.

## 1. Introduction

One of the basic problems in the theoretical study of the static and dynamic properties of liquid metals has been the non-availability of reliable interatomic potentials. However, the situation is much better for inert gases and simple metals like alkali metals. Lennard-Jones potentials and Aziz potentials have been used extensively in the analysis of the properties of inert gases. These potentials have simple analytic forms and, in dimensionless units, depend only on the distance of separation. Thus they scale as we move from one inert gas to another. However, scaling features can be present even for complex potential forms. For the alkali metals, an effective ion–ion interaction has been obtained to provide reasonable descriptions of their properties in the solid phase as well as in the liquid phase [1–9]. Recently Balucani *et al* [8] have made a very comprehensive computer simulation study of liquid alkali metals near their respective melting points using the potential obtained by Price *et al* [2]. An interesting feature of these potentials, as noted by Balucani *et al*, is their smooth scaling behaviour as one moves from one alkali metal to another. In addition, they demonstrate that static properties, such as the pair correlation function, and dynamic properties, such as the velocity correlation function and peak positions of the longitudinal current correlation function, of liquid alkali metals exhibit scaling features and are in close agreement with available experimental data [10, 11].

Even though our understanding of the broad features of the time correlation functions has increased considerably, it is still not possible to calculate the desired correlation function readily using microscopic theory. Therefore one resorts to the use of models based on physical considerations. A simple model has been proposed by Tankeshwar *et al* [12] to calculate the velocity auto-correlation function and related properties. This model, when applied to Lennard–Jones (LJ), Yukawa and Coulomb fluids, has given remarkably good results, even at the triple point for LJ fluids. In this paper we apply this model for liquid alkali

† Permanent address: Department of Physics, Panjab University, Chandigarh, India 160014.

0953-8984/94/071309+10$07.50 

metals to calculate the velocity auto-correlation function, its frequency spectrum along with the associated memory function and the self-diffusion coefficient, using, as inputs, only the interatomic potential and the corresponding pair correlation function. The predicted results are compared with recent computer simulation data. A comparison of our results with those of molecular dynamics (MD) and experiments indicates an overall good agreement.

In section 2 we present the necessary theoretical framework of the model and the results are given in section 3.

## 2. Theoretical framework

The normalized velocity auto-correlation function (VACF), denoted by $\psi(t)$, is defined as

$$\psi(t) = \langle v_{1x}(0)v_{1x}(t)\rangle/v_0^2 \tag{1}$$

where $v_{1x}(t)$ is the $x$ component of the velocity of particle 1 at time $t$. The system consists of $N$ identical particles interacting with a pair potential $u(r)$. $v_0 = (k_B T/M)^{1/2}$ is the thermal speed of the particle. Denoting

$$\tilde{\psi}(z) = \mathrm{i}\int_0^\infty \mathrm{e}^{\mathrm{i}zt}\psi(t)\,\mathrm{d}t \qquad \text{with } z = \omega + \mathrm{i}0^+$$

as the Fourier–Laplace transform of the VACF, we have the Mori–Zwanzig representation

$$\tilde{\psi}(z) = -1/(z + \tilde{K}(z)) \tag{2}$$

with the memory function $\tilde{K}(z) = K'(\omega) + \mathrm{i}K''(\omega)$. We readily obtain the memory function in the time domain from

$$K(t) = \frac{2}{\pi}\int_0^\infty K''(\omega)\cos(\omega t)\,\mathrm{d}\omega \tag{3}$$

with

$$K''(\omega) = \psi''(\omega)/\{[\psi'(\omega)]^2 + [\psi''(\omega)]^2\} \tag{4}$$

where $-\psi'(\omega)$ and $\psi''(\omega)$ are the sine and cosine transforms of $\psi(t)$. The frequency spectrum of the VACF, denoted by $f(\omega)$, is equal to $2\psi''(\omega)$ and the diffusion coefficient $D$ is given by

$$D/v_0^2 = f(0)/2 = \psi''(\omega = 0). \tag{5}$$

In this work we calculate the VACF directly and the memory function is then obtained later using equations (3) and (4). In order to have a self-contained presentation we briefly recall the essential points of the model. The configuration space of an $N$-particle system is considered to consist of a number of cells characterized by some fixed configurations, determined by the local minima in the potential energy hyper-surface of the system. The particles jump from one cell to another with a jump frequency $a$. The effect of the cell jump is to rearrange the equilibrium position of the particles. Within the cell, the particles execute harmonic oscillations, given by $\cos(bt)$, with a fixed frequency $b$. The waiting time distribution for the cell jump is assumed to be given by $\mathrm{sech}(at)$. This choice of the waiting

time distribution provides more jumps at smaller times than at larger times. The motion of the particles in different cells is assumed to be uncorrelated. With the above assumptions, the equilibrium ensemble average in equation (1) can be easily evaluated to yield

$$\psi(t) = \operatorname{sech}(at)\cos(bt). \tag{6}$$

The details of the calculation and the essential differences between our model and the earlier models of Zwanzig [13] and Mohanty [14] have been discussed in [10]. The parameters $a$ and $b$ are determined using the short-time properties of $\psi(t)$. We then have

$$a = \sqrt{\delta_2}/2 \qquad b = \sqrt{4\delta_1 - \delta_2}/2 \tag{7}$$

where

$$\delta_1 = A = \frac{4\pi n}{3m}\int_0^\infty \mathrm{d}r r^2 g(r)\left(\frac{2}{r}u_1 + u_2\right) \tag{8}$$

and

$$\delta_2 = B/A - A \tag{9}$$

with

$$B = \frac{8\pi n}{3m^2}\int_0^\infty \mathrm{d}r r^2 g(r)\left(\frac{2}{r^2}u_1^2 + u_2^2\right) + \frac{8\pi^2 n^2}{3m^2}\int_0^\infty\int_0^\infty \mathrm{d}r\,\mathrm{d}r' r^2 r'^2 \times \int_{-1}^{1}\mathrm{d}\mu g_3(r, r')\left[\mu^2 u_2 u_2' + \frac{(1+\mu^2)}{rr'}u_1 u_1' + \frac{2(1-\mu^2)}{r'}u_2 u_1'\right]. \tag{10}$$

In equations (8) and (10) $u_1 = \mathrm{d}u(r)/\mathrm{d}r$, $u_2 = \mathrm{d}^2u(r)/\mathrm{d}r^2$ and the corresponding prime quantities denote derivatives with respect to the prime variable $r'$. $g(r)$ and $g_3(r, r')$ are the static pair, and triplet correlation function. For the latter, we use the Kirkwood superposition approximation in the evaluation of these integrals. $A$ and $B$ are essentially the coefficients of $t^2$ and $t^4$ in the time expansion of the VACF.

It is easy to obtain analytical expressions for $\psi'(\omega)$ and $\psi''(\omega)$ using equation (6). They are given by

$$\psi'(\omega) = \frac{\pi}{4a}\left[\tanh\frac{\pi}{2a}(\omega + b) + \tanh\frac{\pi}{2a}(\omega - b)\right] - 2\sum_{k=0}^{\infty}\left[\frac{\omega + b}{(\omega + b)^2 + a^2(1+4k)^2} + \frac{\omega - b}{(\omega - b)^2 + a^2(1+4k)^2}\right] \tag{11}$$

$$\psi''(\omega) = (\pi/4a)[\operatorname{sech}(\pi/2a)(\omega + b) + \operatorname{sech}(\pi/2a)(\omega - b)]. \tag{12}$$

Thus we have a simple expression for the self-diffusion coefficient $D$ given by

$$D = (\pi/2a)v_0^2\operatorname{sech}(\pi b/2a). \tag{13}$$

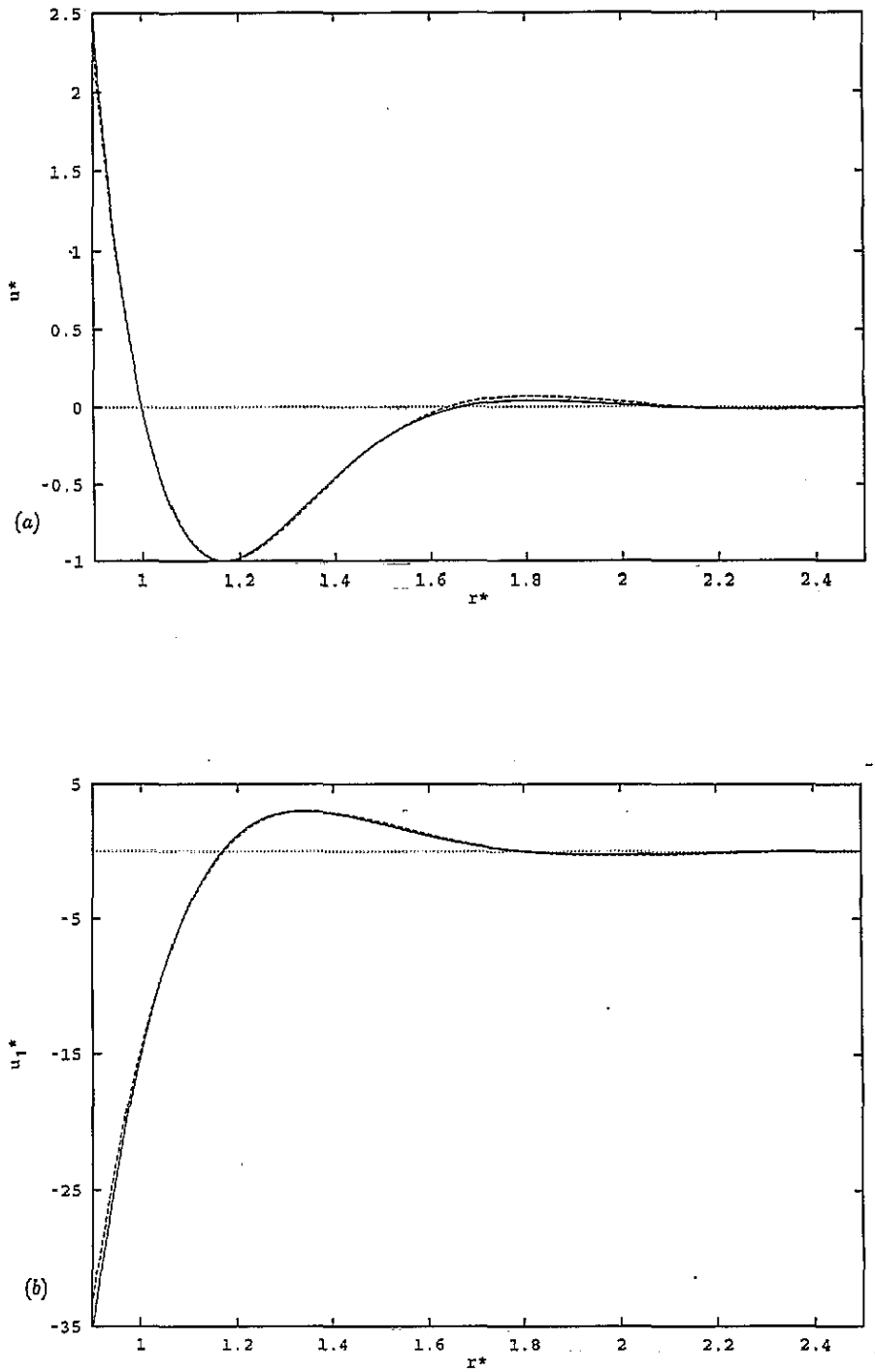


**Figure 1.** The PST interatomic potential $u^* = u(r)/\epsilon$ and its first three derivatives $u_1^*$, $u_2^*$ and $u_3^*$ are plotted in (*a*), (*b*), (*c*) and (*d*), respectively, as a function of $r^* = r/\sigma$. The full curve is for Na and the broken curve is for Cs. The corresponding curves for K and Rb lie between those of Na and Cs. The densities correspond to a reduced density of $n^* = 0.895$, at their melting temperatures.

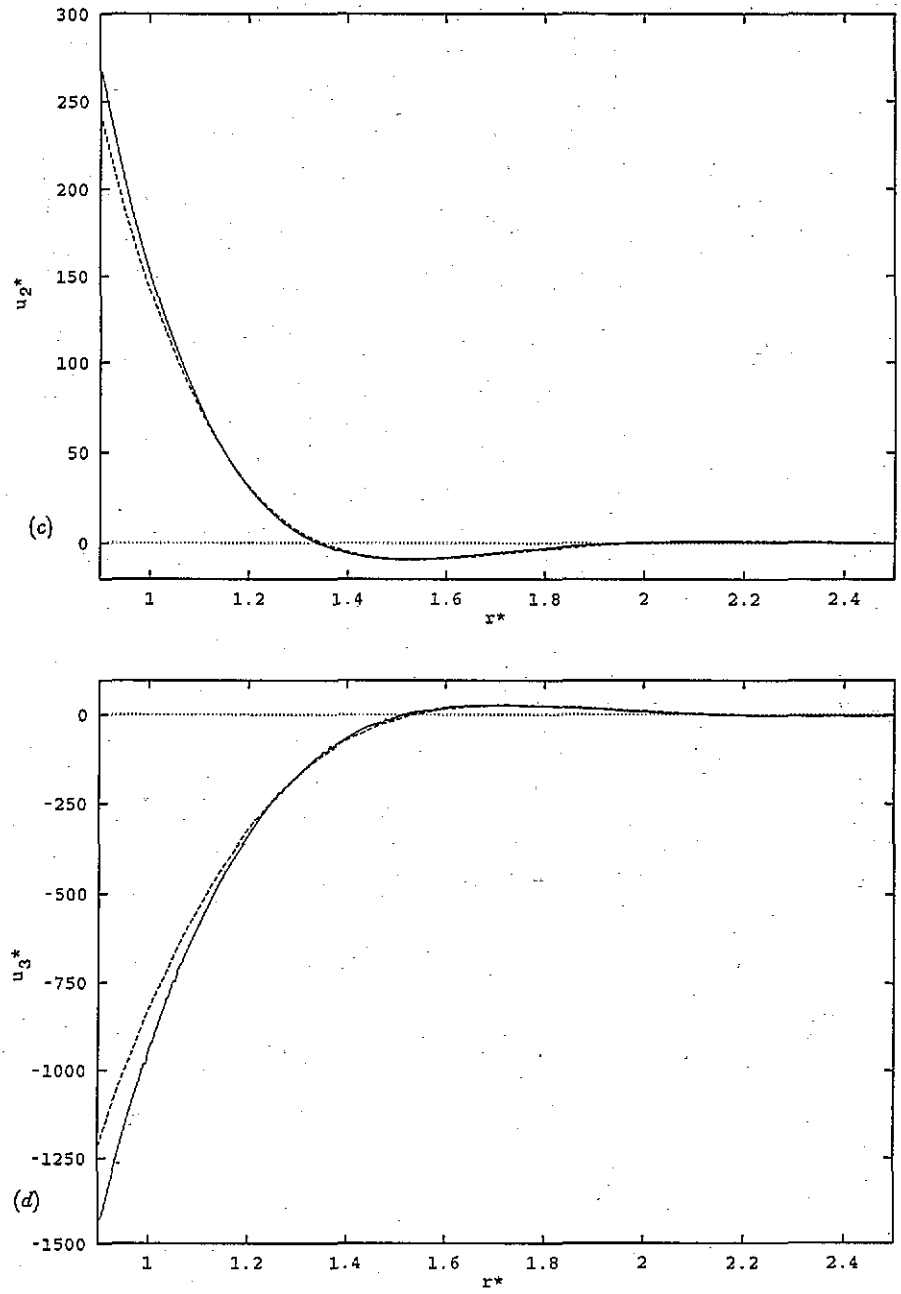


**Figure 1.** (Continued)

## 3. Results and discussion

In order to obtain numerical results, we only need values for $A$ and $B$, which are easily obtained once the potential and its corresponding $g(r)$ is known. For liquid alkali metals, we have used the potentials of Price, Singwi and Tosi [2] (PST) and the corresponding

$g(r)$ obtained by Balucani *et al* by computer simulation [8]. It should be noted that PST potentials are not true potentials, but only effective pair potentials. They depend not only on the distance of separation, but also on other factors such as the density (and hence the temperature). The many-body effects in PST potentials enter through the parameters of the potential and we refer the reader to their paper [2] for further details.

In figure 1 we have plotted $u^* = u(r)/\epsilon$ and its first three derivatives as a function of $r^* = r/\sigma$ where $\epsilon$ is the potential well depth and $\sigma$ is the position of the first zero of the potential. For purposes of clarity, only curves for sodium (Na) (full curve) and caesium (Cs) (broken curve) are presented in figures 1($a$)–1($d$). The corresponding curves for potassium (K) and rubidium (Rb) lie between these two curves. The scaling feature of the potential is clearly seen in figure 1($a$). It can be noted from figures 1($b$) to 1($d$) that the scaling behaviour is preserved to a very good approximation in the derivatives also, except for some deviations around $r \simeq \sigma$. The deviations increase with the order of the derivative. The deviations could be partly due to the numerical procedure used and partly due to small differences in the potentials themselves, which get amplified in the derivatives. These deviations may have some effect on the universal behaviour of dynamical correlation functions, especially those involving many-particle dynamics. However, these deviations do not have a significant effect on our results as our model uses only the first two derivatives of the potential.

The numerical results for $A$, which is also the square of the Einstein frequency, and $B$, along with some of the parameters for liquid alkali metals are presented in table 1. It is seen that $A\tau^2$ and $B\tau^4$ are practically the same for rubidium and caesium, where $\tau^2 = m\sigma^2/\epsilon$. The maximum difference is less than 5% for $A\tau^2$ and less than 10% for $B\tau^4$. It should be noted that there is a difference of about 8% in their $T^* = k_B T/\epsilon$ and so the differences in the coefficients $A\tau^2$ and $B\tau^4$ may be due to slight differences in their $T^*$ and in the derivatives of the potentials. Keeping these points in mind, one is tempted to conclude that $A\tau^2$ and $B\tau^4$ do scale. Since $A$ and $B$ are related to the short-time expansion of the VACF, the scaling of these coefficients implies scaling of the VACF, at least for short times.

**Table 1.** Physical parameters and diffusion coefficients $D$ (in units of $10^{-5}$ cm$^2$ s$^{-1}$) for liquid alkali metals. The calculated values are the prediction of our model. $D_{MD}$ and $D_{expt}$ are molecular dynamics and experimental values.

| Metal | $\epsilon$ (K) | $\sigma$ (Å) | $n$ (Å$^{-3}$) | $T$ (K) | $A\tau^2$ | $B\tau^4$ | $D_{cal}$ | $D_{MD}$ | $D_{expt}$ |
|---|---|---|---|---|---|---|---|---|---|
| Li | 567.1 | 2.728 | 0.0441 | 454 | — | — | 6.7 | — | 6.1–6.8 |
| Na | 445.6 | 3.328 | 0.0229 | 376 | 186.5 | 77890 | 4.41 | 4.06 | 4.06–4.35 |
| K | 421.4 | 4.115 | 0.0128 | 343 | 183.6 | 73900 | 3.78 | 3.58 | 3.52–3.72 |
| Rb | 402.2 | 4.408 | 0.0104 | 312 | 178.4 | 69870 | 2.60 | 2.40 | 2.60 |
| Cs | 385.5 | 4.761 | 0.0083 | 302 | 178.3 | 69980 | 2.22 | 2.11 | 2.16 |

Using the parameters for rubidium, we have calculated the VACF, $f(\omega)$, the real and the imaginary parts of the memory function in frequency space and the memory function in the time domain. The VACF is represented in figure 2 as the function $t^* = t/\tau$ by the full curve, while the computer simulation data are represented by the broken curve. Our calculated result reproduces all the well known features of the VACF, such as a negative minimum, a feature also present in Lennard–Jones liquids near the triple point. A distinctive feature of the VACF in liquid metals is the oscillations, which are not reproduced very well by our model. This is to be expected, as it is in this region of the time domain that the model does not correctly incorporate certain physical effects like mode couplings. However the areas

under the two curves, which are related to the diffusion coefficient, are very close. In figure 3 we plot the reduced frequency spectrum $f^*(\omega) = f(\omega)\ \tau/2\sigma^2$ as a full curve. The broken curve is from the computer simulation data. The important features of the MD data are the appearance of a peak at $\omega^* = \omega\tau \simeq 10$ and the flatness of the spectrum from $\omega^* \simeq 11$ to $\omega^* \simeq 14$. Similar features have been seen in the MD data on LJ fluids [15] at the triple point and on liquid caesium using a different potential [16]. The flat region is probably indicative of the onset of a new relaxation mechanism, which is predicted by mode coupling theory in the strong coupling limit for the glassy state [17]. The frequency spectrum obtained from the model only has a peak at $\omega^* \simeq 11$, which is somewhat shifted towards the low-frequency side from the centre of the broad spectrum obtained from computer simulation data. The MD data and the model data are both shifted toward the small-$\omega$ side from the Einstein frequency given by $\omega_E^* = 14.4$. Although there are discrepancies between the two spectra, the model results are satisfactory.

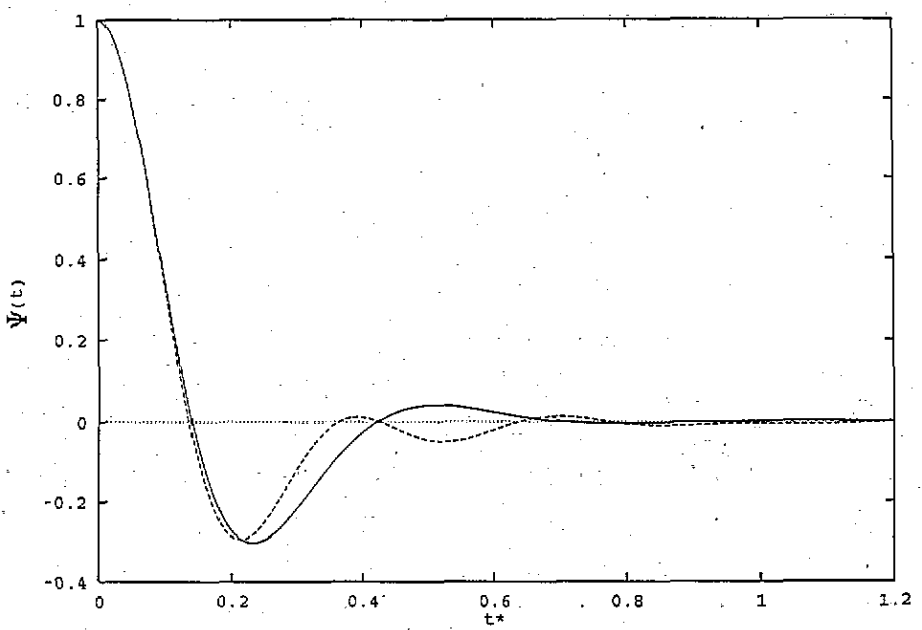


**Figure 2.** The velocity auto-correlation function as a function of $t^* = t/\tau$. The model results and computer simulation data are shown as a full and broken curve, respectively.

A quantity of theoretical interest is the memory function of the VACF. Although our model does not require a memory function in its formulation, we have extracted it to see the extent to which it includes the actual memory effects and for comparison with other theoretical calculations. The real and the imaginary parts, $K'(\omega)/\tau$ and $K''(\omega)/\tau$ are plotted in figure 4 as full curves. The computer simulation results are shown as broken curves. The top portion (positive $y$-axis) of the figure denotes the imaginary part. It is interesting to note that our simple model is in semi-quantitative agreement with the simulation data. The memory function in time space, calculated from equations (3) and (4), is plotted in figure 5. The slight differences for $t^* < 0.1$ could be partly due to the use of the superposition approximation in our calculations. A study of this figure indicates that the model memory function has a tendency to show a minimum around $t^* \simeq 0.2$ but the effect is small. A

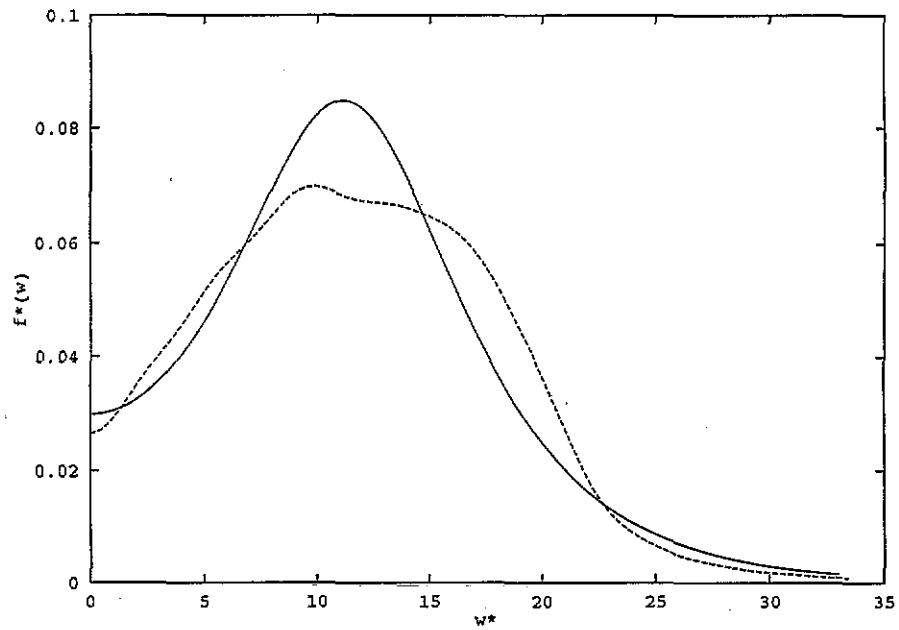


**Figure 3.** The reduced frequency spectrum versus $\omega^* = \omega\tau$. The curves are as in figure 2.

comparison with the mode coupling calculation of Balucani *et al* [8] shows that the present model includes more than the binary collision effects estimated by them. Further, even the mode coupling calculations do not account for the minimum seen in the MD memory function. Although there are differences between the memory function obtained from the computer simulation data of the VACF and that of the model, they are within a respectable range.

It is clear from figures 2 to 5 that, while there is an overall good agreement between our model results and the computer simulation results, there are small deviations even at short times, and thus our model does not reproduce all of the short-time responses exactly. We believe that these deviations could partly be attributed to the details of the binary collisions. Especially for a continuous potential, like the PST potential, these effects cannot be modelled exactly and our model accounts for these collisions only in some average way.

The calculated diffusion coefficient from equation (5) is given in table 1 along with molecular dynamics [8] and experimental values [18, 19]. The dimensionless diffusion coefficients $D^* = D\tau/\sigma^2$ are found to be 0.033, 0.031, 0.030 and 0.030 for the liquid metals Na, K, Rb and Cs, respectively. Thus only for liquid sodium does there appear to be a slight departure from a universal value. Taking the universal value for $D^*$ to be 0.030, we can predict the diffusion coefficient of liquid lithium, assuming $T^* = 0.8$ and $n^* = n\sigma^3 = 0.895$, and the result is presented in table 1. It is seen that predicted results are in remarkably good agreement with both the MD data and experimental results for all the liquid alkali metals.

In summary, we have used a simple model of atomic motion in liquids to calculate the velocity auto-correlation function, its frequency spectrum, the associated memory function and the self-diffusion coefficients of liquid alkali metals at their melting points. The interatomic potential of Price, Singwi and Tosi, and the corresponding pair correlation function have been used to obtain the two parameters, $a$ and $b$, introduced in the model.

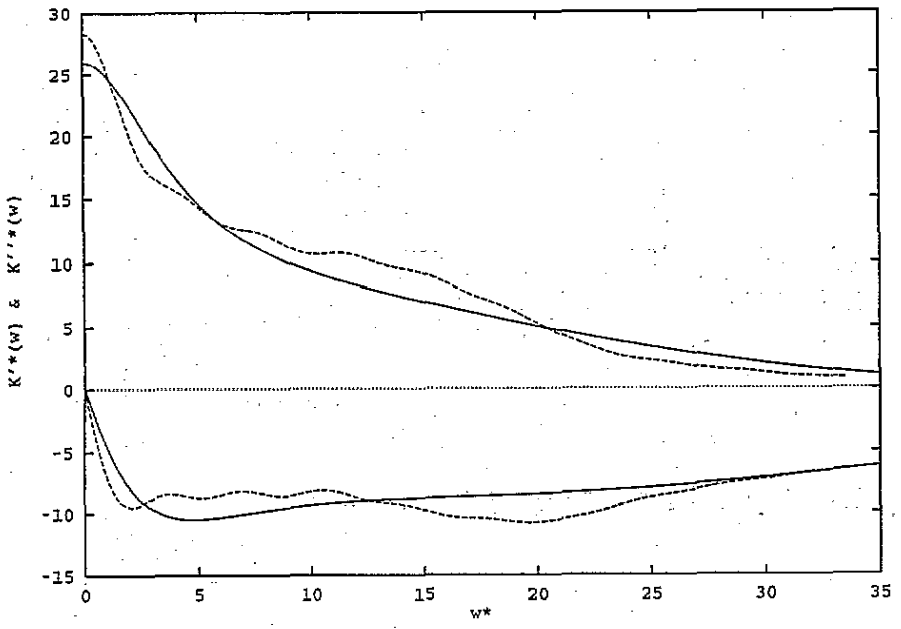


**Figure 4.** The real part $K'(\omega)$ and the imaginary part $K''(\omega)$ of the reduced memory function versus $\omega^*$ with curves as in figure 3. The real part is plotted in the lower portion.

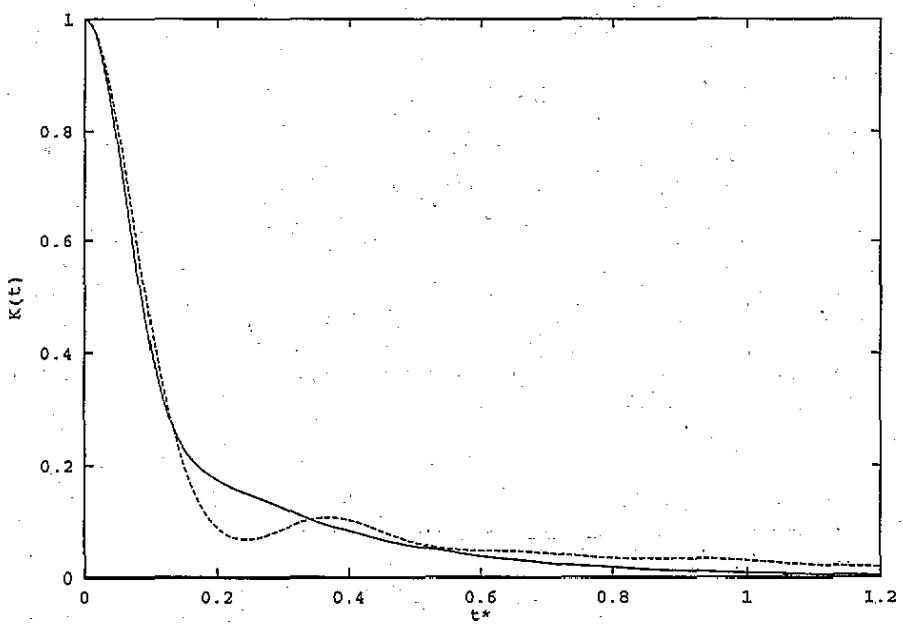


**Figure 5.** The memory function, normalized to unity at $t = 0$, is plotted as a function of the reduced time $t^*$ with the curves as in figure 2.

The predicted results are compared with recent MD data and found to be in overall

good agreement. The self-diffusion coefficients seem to scale nicely when expressed in dimiensionless units determined by their mass and the $\epsilon, \sigma$ parameters of the interatomic potential. It is gratifying to note that a very simple model predicts values for the self-diffusion coefficient for all liquid alkali metals, including lithium, which are in very good agreement with experimental results. The model not only provides acceptable values for the diffusion coefficient but also reproduces essential features of atomic motion in liquid alkali metals. Similar conclusions were arrived at when this model was applied to Lennard–Jones, Yukawa and Coulomb fluids [12]. Therefore, it is hoped that this model would be useful in estimating the self-diffusion coefficients of other systems.

## Acknowledgments

We are very grateful to Dr A Torcini for providing us with the computer simulation data that formed the basis of the present work. One of us (KNP) acknowledges the partial support of the University Grants Commission, New Delhi, through a research project. This work is supported in part by a grant (ARP-FUHEM) from the Department of National Defence, Canada.

## References

[1] Hafner J 1987 *From Hamiltonian to Phase Diagram* (Berlin: Springer)
[2] Price D L, Singwi K S and Tosi M P 1970 *Phys. Rev.* B **2** 2983
[3] Rahman A 1974 *Phys. Rev.* A **9** 1667
[4] Cohen S S, Klein M L, Duesberry M S and Taylor R 1976 *J. Phys. F: Met. Phys.* **6** L27
[5] Dagens L, Rasolt M and Taylor R 1975 *Phys. Rev.* B **11** 2726
[6] Rasolt M and Taylor R 1975 *Phys. Rev.* B **11** 2717
[7] Taylor R and MacDonald A H 1980 *J. Phys. F: Met. Phys.* **10** 2387
[8] Balucani V, Torcini A and Vallauri R 1992 *Phys. Rev.* A **46** 2159
[9] Kambayashi S and Kahl G 1992 *Phys. Rev.* A **46** 3255
[10] Copley J R D and Rowe J M 1972 *Phys. Rev.* A **9** 1656
[11] Bodenstainer T, Morkel P, Glaser J and Dorner B 1992 *Phys. Rev.* A **45** 5709
[12] Tankeshwar K, Singla B and Pathak K N 1991 *J. Phys.: Condens. Matter* **3** 3173
[13] Zwanzig R 1983 *J. Chem. Phys.* **79** 4507
[14] Mohanty U 1985 *Phys. Rev.* A **32** 3055
[15] Rahman A 1964 *Phys. Rev.* **136** A405
[16] Ranganathan S, Pathak K N and Varshni Y P 1994 *Phys. Rev.* E **49** accepted for publication
[17] Gotze W and Sjogren L 1992 *Rep. Prog. Phys.* **55** 241
[18] Gerl M and Brason A 1985 *Handbook of Thermodynamic and Transport Properties of Alkali Metals* ed R W Ohse (Oxford: Blackwell Scientific) p 845
[19] Protopapas P, Andersen H C and Parlee N A D 1973 *J. Chem. Phys.* **59** 15